

CORONAVIRUS

Preexisting and de novo humoral immunity to SARS-CoV-2 in humans

Kevin W. Ng^{1*}, Nikhil Faulkner^{1*}, Georgina H. Cornish^{1*}, Annachiara Rosa^{2*}, Ruth Harvey³, Saira Hussain³, Rachel Ulferts⁹, Christopher Earl⁴, Antoni G. Wrobel⁵, Donald J. Benton⁵, Chloe Rouston⁶, William Bolland¹, Rachael Thompson¹, Ana Agua-Doce⁷, Philip Hobson⁷, Judith Heaney¹³, Hannah Rickman¹³, Stavroula Paraskevopoulou¹³, Catherine F. Houlihan^{13,14}, Kirsty Thomson¹³, Emilie Sanchez¹³, Gee Yen Shin¹³, Moira J. Spyer^{13,15}, Dhira Joshi⁸, Nicola O'Reilly⁸, Philip A. Walker⁶, Svend Kjaer⁶, Andrew Riddell⁷, Catherine Moore¹⁶, Bethany R. Jebson^{17,19}, Meredith Wilkinson^{17,19}, Lucy R. Marshall^{17,19}, Elizabeth C. Rosser^{17,18}, Anna Radziszewska^{17,18}, Hannah Peckham^{17,18}, Coziana Ciurtin^{17,18}, Lucy R. Wedderburn^{17,19}, Rupert Beale⁹, Charles Swanton¹⁰, Sonia Gandhi¹¹, Brigitta Stockinger¹², John McCauley³, Steve J. Gamblin⁵, Laura E. McCoy¹⁴†, Peter Cherepanov²†, Eleni Nastouli^{13,15}†, George Kassiotis^{1,20}†

Zoonotic introduction of novel coronaviruses may encounter preexisting immunity in humans. Using diverse assays for antibodies recognizing SARS-CoV-2 proteins, we detected preexisting humoral immunity. SARS-CoV-2 spike glycoprotein (S)-reactive antibodies were detectable using a flow cytometry-based method in SARS-CoV-2-uninfected individuals and were particularly prevalent in children and adolescents. They were predominantly of the immunoglobulin G (IgG) class and targeted the S2 subunit. By contrast, SARS-CoV-2 infection induced higher titers of SARS-CoV-2 S-reactive IgG antibodies targeting both the S1 and S2 subunits, and concomitant IgM and IgA antibodies, lasting throughout the observation period. SARS-CoV-2-uninfected donor sera exhibited specific neutralizing activity against SARS-CoV-2 and SARS-CoV-2 S pseudotypes. Distinguishing preexisting and de novo immunity will be critical for our understanding of susceptibility to and the natural course of SARS-CoV-2 infection.

Immune cross-reactivity among seasonally spreading human coronaviruses (HCoVs) has long been hypothesized to provide effective but transient cross-protection against distinct HCoVs (1, 2). To determine the degree of cross-reactivity between HCoVs and SARS-CoV-2, we developed a flow cytometry-based assay for SARS-CoV-2-binding antibodies. The main target for such antibodies is the spike glycoprotein (S), which is proteolytically processed into the S1 and S2 subunits, mediating target cell attachment and entry, respectively.

The S1-specific CR3022 antibody stained a smaller percentage of SARS-CoV-2 S-expressing human embryonic kidney (HEK) 293T cells and with lower intensity than COVID-19 convalescent sera (fig. S1), indicating that polyclonal immunoglobulin G (IgG) antibodies targeted a wider range of epitopes naturally processed and displayed on these cells. This assay also detected SARS-CoV-2 S-reactive IgM and IgA antibodies in COVID-19 convalescent sera

(fig. S2). Indeed, the presence of SARS-CoV-2 S-reactive antibodies of all three Ig classes (IgG⁺IgM⁺IgA⁺) distinguished COVID-19 sera from control sera with a high degree of sensitivity and specificity (Fig. 1A and fig. S3). All 156 seroconverted COVID-19 patients had contemporaneous IgG, IgM, and IgA responses to SARS-CoV-2 S throughout the observation period, with the exception of two patients who only had IgG antibodies (figs. S4 and S5). One of these patients was a bone marrow transplantation recipient who experienced HCoV infection 1 month before SARS-CoV-2 infection (fig. S6). Unexpectedly, a small proportion of SARS-CoV-2-uninfected patients sampled before or during the early spread of SARS-CoV-2 in the United Kingdom (table S1) also had SARS-CoV-2 S-binding IgG antibodies, but not IgM or IgA antibodies (Fig. 1A), suggesting the presence of cross-reactive immunological memory.

The S2 subunit exhibits a higher degree of homology among coronaviruses than S1 (fig.

S7) and was likely the main target of cross-reactive antibodies. Competition with recombinant soluble S1 or S2 at doses that blocked binding of specific monoclonal antibodies (fig. S8) did not affect the frequency of cells stained with COVID-19 patient sera, although the intensity of staining was reduced by 31 and 37%, respectively (Fig. 1, B to D), indicating recognition of both S1 and S2. By contrast, soluble S2 completely abolished staining with SARS-CoV-2-uninfected patient sera, whereas soluble S1 had no effect (Fig. 1, B to D). Thus, SARS-CoV-2-uninfected patient sera cross-react with SARS-CoV-2 S2, and COVID-19 patient sera additionally recognize S1.

SARS-CoV-2 S-reactive IgG antibodies were detected by flow cytometry in five of 34 SARS-CoV-2-uninfected individuals with HCoV infection confirmed by reverse transcription-quantitative polymerase chain reaction, as well as in one of 31 individuals without recent HCoV infection (Fig. 2A and fig. S4A). This suggested that cross-reactivity may have persisted from earlier HCoV infections rather than having been induced by the most recent one.

To confirm antibody cross-reactivity using an independent assay, we developed enzyme-linked immunosorbent assays (ELISAs) using recombinant SARS-CoV-2-stabilized trimeric S ectodomain, S1, receptor-binding domain (RBD), or nucleoprotein (N). Rates of IgG seropositivity by SARS-CoV-2 S1-coated ELISA were congruent with, but generally lower than, those by flow cytometry (fig. S9). The three SARS-CoV-2-uninfected individuals with the highest cross-recognition of S by flow cytometry, plus an additional four individuals, had ELISA-detectable IgG antibodies against the SARS-CoV-2 S ectodomain, as well as N (Fig. 2A and fig. S4, B to D). By contrast, none of the control samples had ELISA-detectable IgG antibodies against the less-conserved SARS-CoV-2 S1 or RBD (Fig. 2A and fig. S4, B to D).

The prevalence of such cross-reactive antibodies was further examined in additional healthy donor cohorts (table S1). Among 50 SARS-CoV-2-uninfected pregnant women sampled in May of 2018, five showed evidence for SARS-CoV-2 S-reactive IgG antibodies, but not IgM or IgA antibodies (Fig. 2B and fig.

¹Retroviral Immunology, The Francis Crick Institute, London NW1 1AT, UK. ²Chromatin Structure and Mobile DNA Laboratory, The Francis Crick Institute, London NW1 1AT, UK. ³Worldwide Influenza Centre, The Francis Crick Institute, London NW1 1AT, UK. ⁴Signalling and Structural Biology Laboratory, The Francis Crick Institute, London NW1 1AT, UK. ⁵Structural Biology of Disease Processes Laboratory, The Francis Crick Institute, London NW1 1AT, UK. ⁶Structural Biology STP, The Francis Crick Institute, London NW1 1AT, UK. ⁷Flow Cytometry STP, The Francis Crick Institute, London NW1 1AT, UK. ⁸Peptide Chemistry, The Francis Crick Institute, London NW1 1AT, UK. ⁹Cell Biology of Infection Laboratory, The Francis Crick Institute, London NW1 1AT, UK. ¹⁰Cancer Evolution and Genome Instability Laboratory, The Francis Crick Institute, London NW1 1AT, UK. ¹¹Neurodegeneration Biology Laboratory, The Francis Crick Institute, London NW1 1AT, UK. ¹²AhRimmunity Laboratory, The Francis Crick Institute, London NW1 1AT, UK. ¹³University College London Hospitals (UCLH) NHS Trust, London NW1 2BU, UK. ¹⁴Division of Infection and Immunity, University College London (UCL), London WC1E 6BT, UK. ¹⁵Department of Population, Policy and Practice, Great Ormond Street Institute for Child Health (ICH), UCL, London WC1N 1EH, UK. ¹⁶Public Health Wales, University Hospital of Wales, Cardiff CF14 4XW, UK. ¹⁷Centre for Adolescent Rheumatology Versus Arthritis at UCL, UCLH, Great Ormond Street Hospital (GOSH), London WC1N 3JH, UK. ¹⁸Centre for Rheumatology Research, Division of Medicine, UCL, London, WC1E 6BT, UK. ¹⁹UCL Great Ormond Street Institute for Child Health (ICH), UCL, London WC1N 1EH, UK. ²⁰Department of Medicine, Faculty of Medicine, Imperial College London, London W2 1PG, UK.

*These authors contributed equally to this work.

†Corresponding author. Email: george.kassiotis@crick.ac.uk (G.K.); e.nastouli@ucl.ac.uk (E.N.); peter.cherepanov@crick.ac.uk (P.C.); l.mccoy@ucl.ac.uk (L.E.M.)

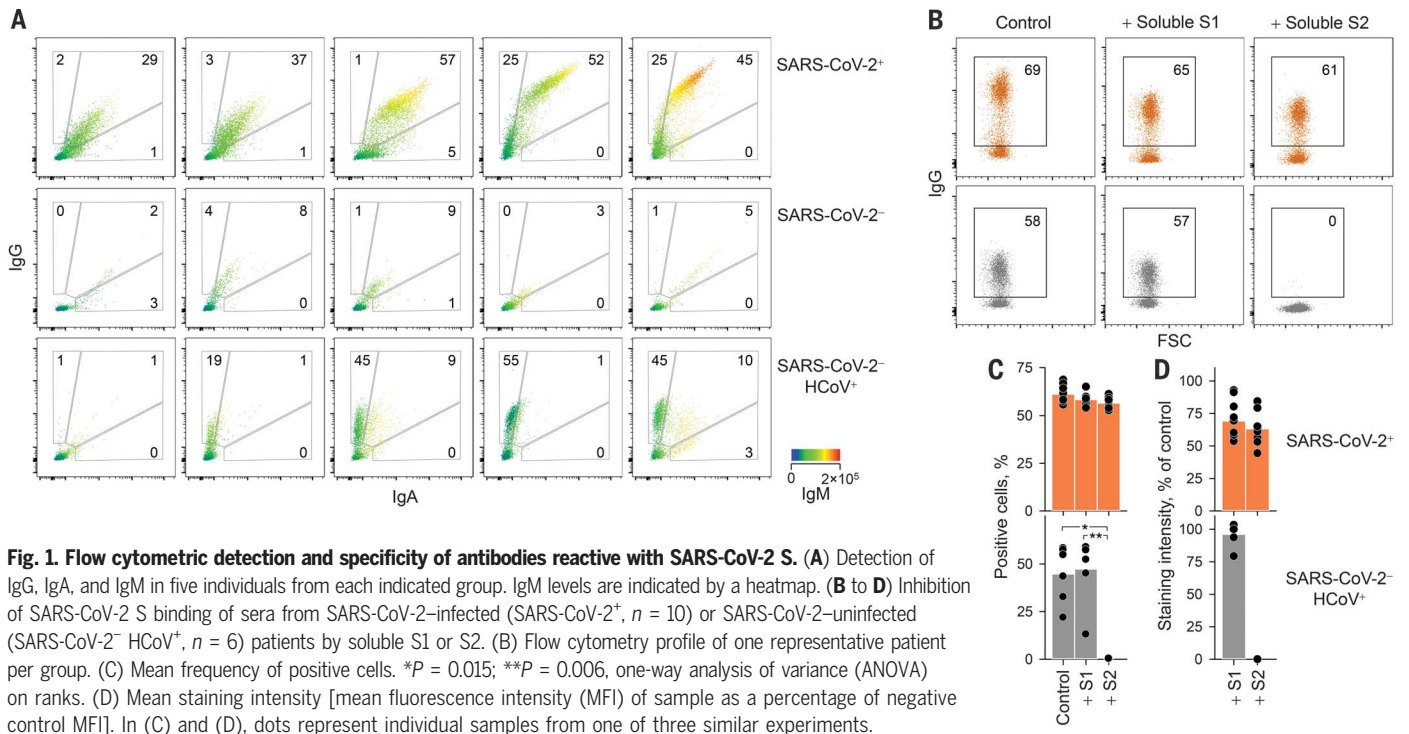
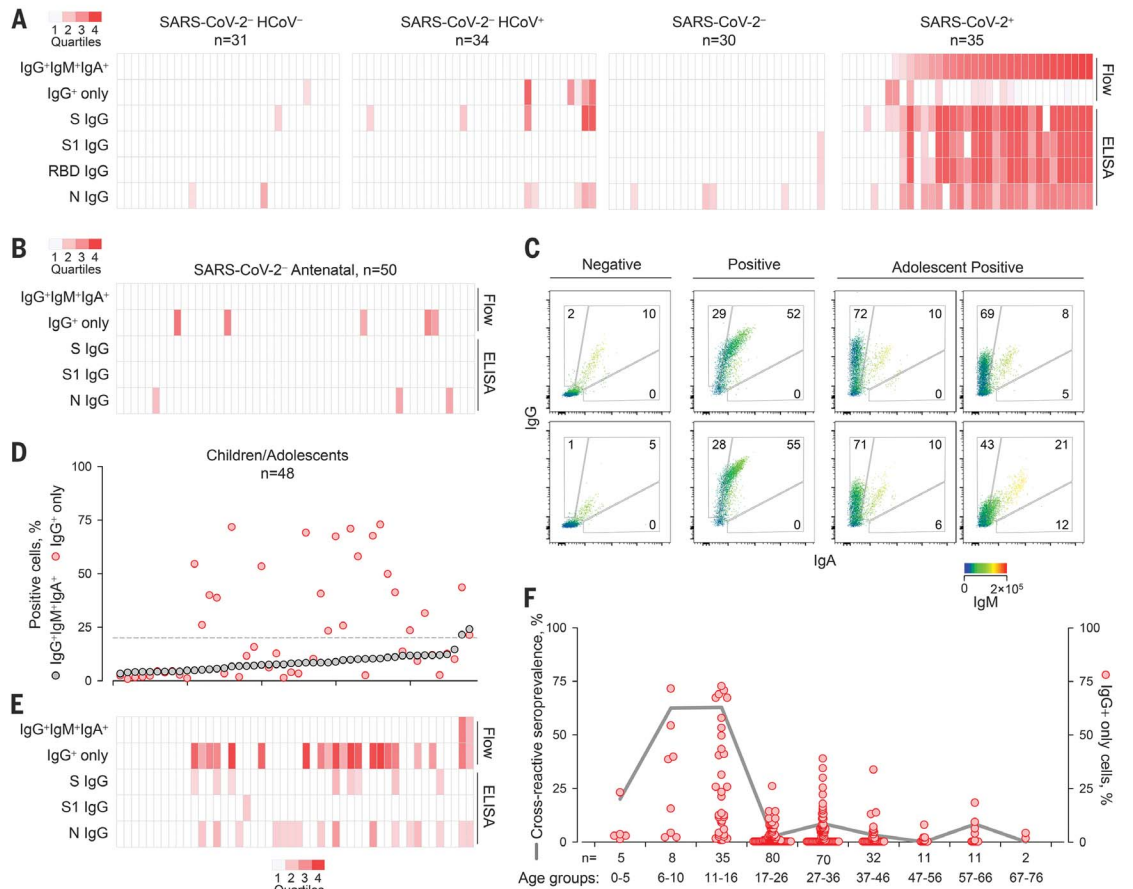


Fig. 2. Prevalence of SARS-CoV-2 S-cross-reactive antibodies detected by different methods.

(A) Flow cytometry and ELISA results for each sample in cohorts A and C to E listed in table S1. (B) Flow cytometry and ELISA results for serum samples from SARS-CoV-2-uninfected pregnant women. (C to E) SARS-CoV-2 S-cross-reactive antibodies in healthy children and adolescents. (C) Representative flow cytometry profiles of seronegative donors (Negative) or COVID-19 patients (Positive) and of SARS-CoV-2-uninfected adolescents with SARS-CoV-2 cross-reactive antibodies. (D) Frequency of cells stained with all three antibody classes (IgG⁺IgM⁺IgA⁺) or only with IgG (IgG⁺) ranked by their IgG⁺IgM⁺IgA⁺ frequency. The dashed line denotes the assay sensitivity cutoff. (E) Flow cytometry and ELISA results for each sample. (F) Prevalence of SARS-CoV-2 S-cross-reactive antibodies in the indicated age groups (line) and frequency of cells that stained only with IgG (dots) in all samples for which the date of birth was known. The heatmaps in (A), (B), and (E) represent the quartile values above each assay's technical cutoff.



S10). In a separate cohort of 101 SARS-CoV-2-uninfected donors sampled in May of 2019, three had SARS-CoV-2 S-reactive IgG antibodies (fig. S11) that did not correlate with antibodies to the diverse viruses and bacteria also present in several of these samples.

SARS-CoV-2 S-reactive IgM and IgA were also detected in two of these donors, albeit at considerably lower levels than in COVID-19 patients (fig. S11), suggestive of recent or ongoing response. In an additional cohort of 13 donors recently infected with HCoVs, only one

had SARS-CoV-2 S-reactive IgG antibodies, and these were at very low levels (fig. S12). This suggested that their emergence was not simply a common transient event after each HCoV infection in this age group (median age 51 years; table S1). Instead, given that HCoV-reactive antibodies are present in virtually all adults (3–5), the rarity of SARS-CoV-2 S cross-reactivity (16 of 302; 5.29%) indicates additional requirements such as random B cell receptor repertoire focusing or frequency of HCoV infection rather than time since the last HCoV infection. Indeed, the frequency of HCoV infection displays a characteristic age distribution, being the highest in children and adolescents (1, 4–8). We therefore examined a cohort of younger SARS-CoV-2-uninfected healthy donors (age 1 to 16 years; table S1) sampled between 2011 and 2018. At least 21 of these 48 donors had detectable levels of SARS-CoV-2 S-reactive IgG antibodies (Fig. 2, C to E), whereas only one of an additional cohort of 43 young adults (age 17 to 25 years; table S1) had such antibodies (Fig. 2F). Staining with sera from SARS-CoV-2-uninfected children and adolescents was specific to HEK293T cells expressing SARS-CoV-2 S, but not the unrelated HERV-K113 envelope glycoprotein, and was outcompeted by soluble SARS-CoV-2 S2 (fig. S13). The prevalence of SARS-CoV-2 S-reactive IgG antibodies peaked at 62% between 6 and 16 years of age (Fig. 2F), when HCoV seroconversion in this age group also peaks (3, 4, 6, 7), and was significantly higher than in adults ($P < 0.00001$, Fisher's exact test).

To determine the potential consequences of antibody cross-reactivity, we examined the ability of preexisting antibodies to inhibit SARS-CoV-2 entry into HEK293T cells (fig. S14 and supplementary text). Although not expected to directly inhibit RBD-mediated cell attachment, S2-targeting antibodies that can neutralize SARS-CoV-2 have recently been discovered (9, 10). HEK293T cell infection with SARS-CoV-2 S pseudotypes was efficiently inhibited by sera from seroconverted (Ab^+) COVID-19 patients, but not from those who had not yet seroconverted (Ab^-) (Fig. 3A). Sera from SARS-CoV-2-uninfected donors with SARS-CoV-2 S-reactive antibodies also neutralized these pseudotypes, whereas none of the sera neutralized vesicular stomatitis virus (VSV) glycoprotein pseudotypes (Fig. 3A). Comparable neutralization of SARS-CoV-2 S pseudotypes was also observed with sera from SARS-CoV-2-uninfected adolescents (Fig. 3A). Moreover, most of the sera from SARS-CoV-2-uninfected donors with flow cytometry-detectable cross-reactive antibodies also neutralized authentic SARS-CoV-2 infection of Vero E6 cells, albeit on average less potently than COVID-19 patient sera (Fig. 3B). By contrast, sera from SARS-CoV-2-uninfected patients without cross-reactive antibodies exhibited no

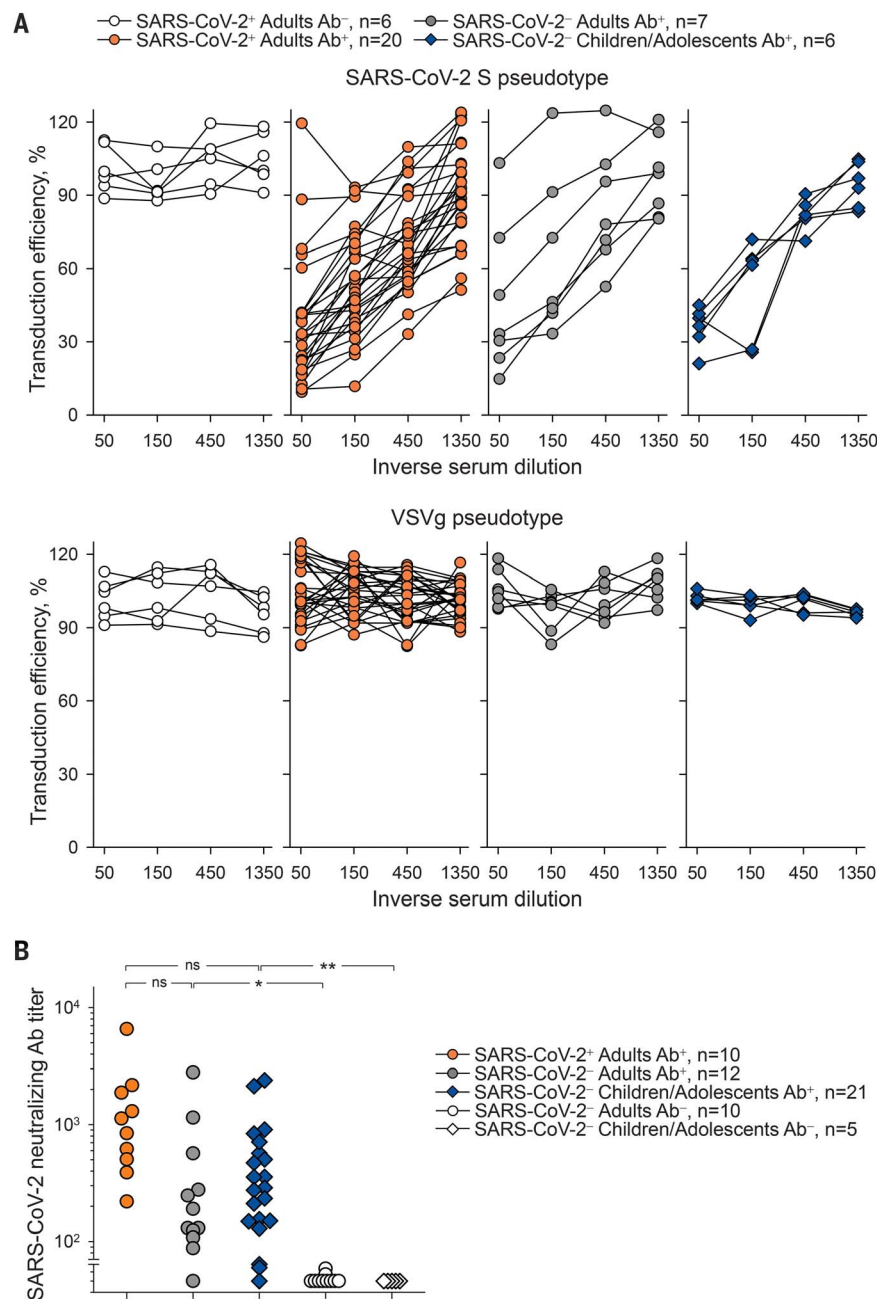
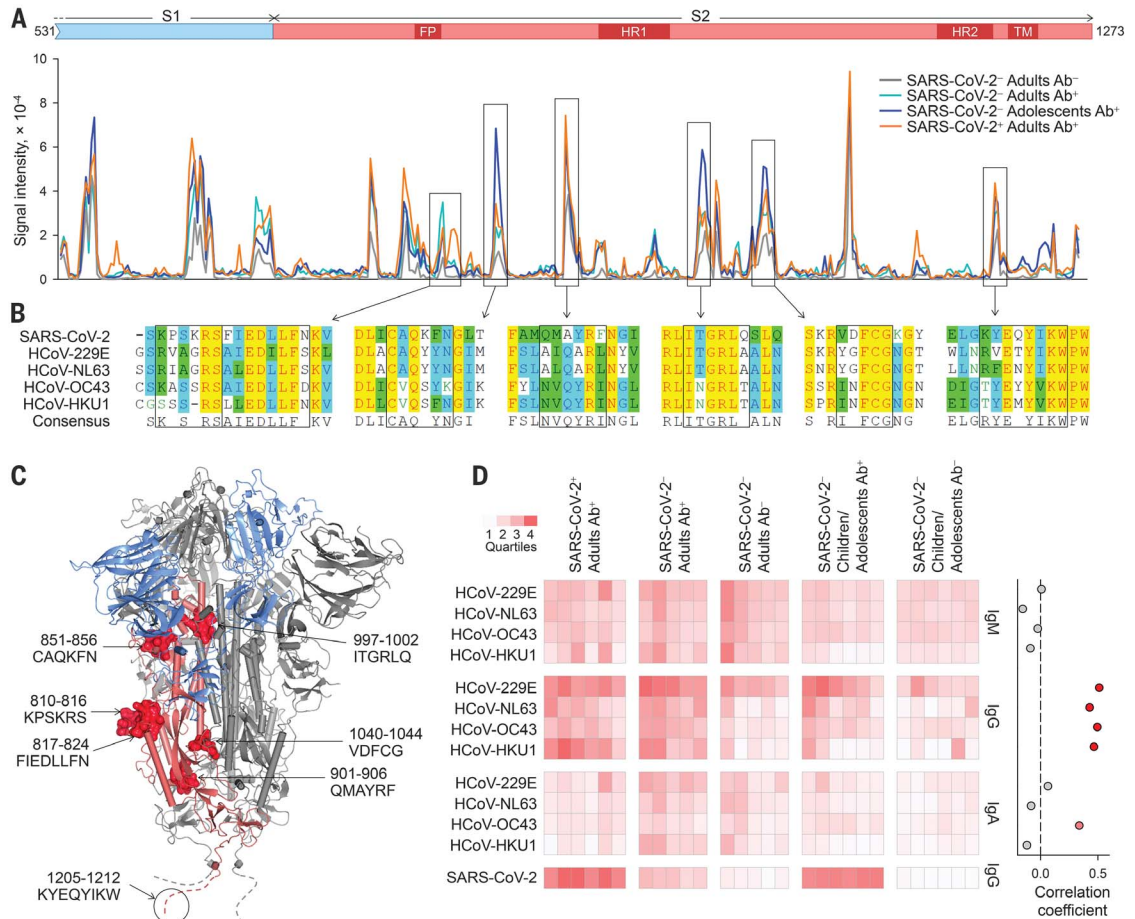


Fig. 3. Neutralization of SARS-CoV-2 S pseudotypes and authentic SARS-CoV-2 by SARS-CoV-2-infected and uninfected patient sera. (A) Inhibition of transduction efficiency of SARS-CoV-2 S or VSVg pseudotypes by adult COVID-19 patients who seroconverted (SARS-CoV-2⁺ Adults Ab⁺) or not (SARS-CoV-2⁻ Adults Ab⁻) and SARS-CoV-2-uninfected adult donors (SARS-CoV-2⁻ Adults Ab⁺) or children and adolescent donors (SARS-CoV-2⁻ Children/Adolescents Ab⁺) with SARS-CoV-2 S-binding antibodies. Each line is an individual serum sample. **(B)** Authentic SARS-CoV-2 neutralization titers of sera from the same donors as in (A), as well as SARS-CoV-2-uninfected donors without SARS-CoV-2 S-binding antibodies (Ab⁻). Dots represent individual samples. * $P = 0.037$; ** $P = 0.014$; ns, not significant by one-way ANOVA on ranks.

Fig. 4. Mapping of cross-reactive epitopes in SARS-CoV-2 S.

(A) Signal intensity for each overlapping peptide along the length of SARS-CoV-2 S covered in the peptide arrays using pooled sera with (Ab⁺) or without (Ab⁻) flow cytometry–detectable SARS-CoV-2 S-reactive antibodies. Differentially recognized peaks are boxed. (B) Alignment of the amino acid sequences of SARS-CoV-2 and HCoV S glycoproteins. Boxes indicate predicted core epitopes. (C) Mapping of predicted epitopes targeted on the trimeric SARS-CoV-2 spike. The S1 (blue) and S2 (pink) subunits of one monomer are colored. Epitopes are shown for one monomer; the circled dashed line represent the membrane proximal region not present in the structure. (D) Left: Reactivity with the S glycoproteins of each HCoV of the indicated sera with (Ab⁺) or without (Ab⁻) flow cytometry–detectable SARS-CoV-2 S-reactive antibodies as determined by flow cytometry. Each column is an individual sample. Rows depict the staining for each antibody class. Right: Correlation coefficients between percentages of IgG staining for SARS-CoV-2 S and IgG, IgM, and IgA staining for each HCoV S glycoprotein.



neutralizing activity (Fig. 3B). Antiviral antibodies may also enhance viral entry by Fc receptor–mediated antibody-dependent enhancement. However, entry of SARS-CoV-2 S pseudotypes was not enhanced by either COVID-19 patient sera or SARS-CoV-2–uninfected patient sera in FcγRIIA-expressing K-562 cells (fig. S15).

Collectively, these findings highlight functionally relevant antigenic epitopes conserved within the S2 subunit. Over its entire length, SARS-CoV-2 S exhibits marginally closer homology with the S proteins of the betacoronaviruses HCoV-OC43 and HCoV-HKU1 than with the alphacoronaviruses HCoV-NL63 and HCoV-229E (fig. S16A). To probe shared epitopes, we constructed overlapping peptide arrays spanning the last 743 amino acids of SARS-CoV-2 S (fig. S16B). Multiple putative epitopes were differentially recognized by sera with cross-reactive antibodies (Ab⁺), were reasonably conserved, and most mapped to the surface of S2 (Fig. 4, A and B, and table S2). An epitope overlapping the S2 fusion peptide was also recently identified as being cross-reactive

with the corresponding peptides from HCoV-OC43 and HCoV-229E (11). Cross-reactivity with the identified epitopes was further supported by ELISAs coated with synthetic peptides (fig. S17).

As expected (3–5), reactivity with one or more HCoVs was detectable by flow cytometry in all sera (Fig. 4D and fig. S18). However, IgG and IgA reactivity against HCoVs was higher in SARS-CoV-2–uninfected adults with SARS-CoV-2–reactive IgG compared with those without ($P = 1.4 \times 10^{-6}$ for IgG and $P = 0.017$ for IgA, Student's *t* test) and in SARS-CoV-2–uninfected children or adolescents with SARS-CoV-2–reactive IgG compared with those without ($P = 0.010$ for IgG and $P = 0.021$ for IgA, Student's *t* test) (Fig. 4D), supporting a direct link between the two. Accordingly, IgG reactivity against each HCoV type was independently correlated with the presence of SARS-CoV-2–reactive antibodies (Fig. 4D).

Our results from multiple independent assays demonstrate the presence of preexisting antibodies recognizing SARS-CoV-2 in uninfected individuals. Identification of conserved

epitopes in S2 targeted by neutralizing antibodies may hold promise for a universal vaccine protecting against current as well as future CoVs. Together with preexisting T cell (12–14) and B cell (10, 15) memory, antibody cross-reactivity between seasonal HCoVs and SARS-CoV-2 may have important ramifications for natural infection. Epidemiological studies of HCoV transmission suggest that cross-protective immunity is unlikely to be sterilizing or long-lasting (8), which is also supported by repeated reinfection (2, 16). Nevertheless, prior immunity induced by one HCoV can reduce the transmission of homologous and heterologous HCoVs and ameliorate the symptoms when transmission is not prevented (1, 2). A possible modification of COVID-19 severity by prior HCoV infection may account for the age distribution of COVID-19 susceptibility, in which higher HCoV infection rates in children than in adults (4, 6) correlate with relative protection from COVID-19 (17) and may also shape seasonal and geographical patterns of transmission. It is imperative that any effect, positive or negative, of preexisting

HCoV-elicited immunity on the natural course of SARS-CoV-2 infection be fully delineated.

REFERENCES

1. R. W. Aldridge *et al.*, *Wellcome Open Res.* **5**, 52 (2020).
2. K. A. Callow, H. F. Parry, M. Sergeant, D. A. Tyrrell, *Epidemiol. Infect.* **105**, 435–446 (1990).
3. E. G. Severance *et al.*, *Clin. Vaccine Immunol.* **15**, 1805–1810 (2008).
4. R. Dijkman *et al.*, *J. Clin. Microbiol.* **46**, 2368–2373 (2008).
5. A. T. Huang *et al.*, *Nat. Commun.* **11**, 4704 (2020).
6. N. Friedman *et al.*, *Viruses* **10**, 515 (2018).
7. S. Nickbakhsh *et al.*, *J. Infect. Dis.* (2020).
8. A. S. Monto *et al.*, *J. Infect. Dis.* **222**, 9–16 (2020).
9. X. Chi *et al.*, *Science* **369**, 650–655 (2020).
10. G. Song *et al.*, bioRxiv 308965 [Preprint]. 23 September 2020; <https://doi.org/10.1101/2020.09.22.308965>.
11. E. Shrock *et al.*, *Science* eabd4250 (2020).
12. A. Grifoni *et al.*, *Cell* **181**, 1489–1501.e15 (2020).
13. J. Braun *et al.*, *Nature* (2020).
14. N. Le Bert *et al.*, *Nature* **584**, 457–462 (2020).
15. P. Nguyen-Contant *et al.*, *mBio* **11**, e01991–e01920 (2020).
16. P. K. Kiyuka *et al.*, *J. Infect. Dis.* **217**, 1728–1739 (2018).
17. R. Castagnoli *et al.*, *JAMA Pediatr.* **174**, 882–889 (2020).

ACKNOWLEDGMENTS

We thank L. James and J. Luptak for the SARV CoV2 N expression construct and M. Pizzato for the SARS CoV2 S cDNA; the entire CRICK COVID-19 Consortium; the Cell Services and High Throughput Screening facilities at the Francis Crick Institute and UCLH Biochemistry (A. Goyale and C. Wilson); and M. Bennet and S. Caidan for training and support in the high-containment laboratory. **Funding:** This work was supported by the Centre of Excellence Centre for Adolescent Rheumatology Versus Arthritis (grant no. 2159), the Great Ormond Street Children's Charity, CureJM Foundation, the NIHR Biomedical Research Centres at GOSH and UCLH, and by the Francis Crick Institute, which receives its core funding from Cancer Research UK, the UK Medical Research Council, and the Wellcome Trust. **Author contributions:** C.C., L.R.W., R.B., C.S., S.G., B.S., J.M., S.J.G., L.E.M., P.C., E.N., and G.K. designed the experiment. K.W.N., N.F., G.H.C., A.Ro., R.H., S.H., R.U., C.E., A.G.W., D.J.B., C.R., W.B., R.T., A.A.-D., P.H., and D.J. performed the investigations. J.H., H.R., S.P., C.F.H., K.T., E.S., G.Y.S., M.J.S., P.A.W., C.M., B.R.J., M.W., L.R.M., E.C.R., A.Ra., and H.P. provided reagents and samples. L.E.M., P.C., E.N., and G.K. wrote the manuscript with contributions from K.W.N., N.F., G.H.C., C.C., and L.R.W. N.O., S.K., A.Ri., C.C., L.R.W., R.B., C.S., S.G., B.S., J.M., S.J.G., L.E.M., P.C., E.N., and G.K. supervised the project. **Competing interests:** The authors declare no competing interests. **Data and materials**

availability: All data are available in the main text or the supplementary materials. This work is licensed under a Creative Commons Attribution 4.0 International (CC BY 4.0) license, which permits unrestricted use, distribution, and reproduction in any medium, provided the original work is properly cited. To view a copy of this license, visit <https://creativecommons.org/licenses/by/4.0/>. This license does not apply to figures/photos/artwork or other content included in the article that is credited to a third party; obtain authorization from the rights holder before using such material.

SUPPLEMENTARY MATERIALS

science.sciencemag.org/content/370/6522/1339/suppl/DC1
Materials and Methods
Supplementary Text
Figs. S1 to S18
Tables S1 and S2
References (18–40)
MDAR Reproducibility Checklist

[View/request a protocol for this paper from Bio-protocol.](#)

31 July 2020; accepted 29 October 2020
Published online 6 November 2020
10.1126/science.abe1107